

Palmitate Diet-induced Loss of Cardiac Caveolin-3: A Novel Mechanism for Lipid-induced Contractile Dysfunction

Catherine J. Knowles, Martina Cebova, Ilka M. Pinz*

Maine Medical Center Research Institute, Maine Medical Center, Scarborough, Maine, United States of America

Abstract

Obesity is associated with an increased risk of cardiomyopathy, and mechanisms linking the underlying risk and dietary factors are not well understood. We tested the hypothesis that dietary intake of saturated fat increases the levels of sphingolipids, namely ceramide and sphingomyelin in cardiac cell membranes that disrupt caveolae, specialized membrane micro-domains and important for cellular signaling. C57BL/6 mice were fed two high-fat diets: palmitate diet (21% total fat, 47% is palmitate), and MCT diet (21% medium-chain triglycerides, no palmitate). We established that high-palmitate feeding for 12 weeks leads to 40% and 50% increases in ceramide and sphingomyelin, respectively, in cellular membranes. Concomitant with sphingolipid accumulation, we observed a 40% reduction in systolic contractile performance. To explore the relationship of increased sphingolipids with caveolins, we analyzed caveolin protein levels and intracellular localization in isolated cardiomyocytes. In normal cardiomyocytes, caveolin-1 and caveolin-3 co-localize at the plasma membrane and the T-tubule system. However, mice maintained on palmitate lost 80% of caveolin-3, mainly from the T-tubule system. Mice maintained on MCT diet had a 90% reduction in caveolin-1. These data show that caveolin isoforms are sensitive to the lipid environment. These data are further supported by similar findings in human cardiac tissue samples from non-obese, obese, non-obese cardiomyopathic, and obese cardiomyopathic patients. To further elucidate the contractile dysfunction associated with the loss of caveolin-3, we determined the localization of the ryanodine receptor and found lower expression and loss of the striated appearance of this protein. We suggest that palmitate-induced loss of caveolin-3 results in cardiac contractile dysfunction via a defect in calcium-induced calcium release.

Citation: Knowles CJ, Cebova M, Pinz IM (2013) Palmitate Diet-induced Loss of Cardiac Caveolin-3: A Novel Mechanism for Lipid-induced Contractile Dysfunction. PLoS ONE 8(4): e61369. doi:10.1371/journal.pone.0061369

Editor: Anita Magdalena Hennige, University of Tübingen, Germany

Received: May 28, 2012; **Accepted:** March 12, 2013; **Published:** April 9, 2013

Copyright: © 2013 Knowles et al. This is an open-access article distributed under the terms of the Creative Commons Attribution License, which permits unrestricted use, distribution, and reproduction in any medium, provided the original author and source are credited.

Funding: This work was supported by the American Heart Association, SDG award 0930260N to IMP, and this work was supported in part by the protein, nucleic acid analysis and cell imaging core facility supported by National Institutes of Health (NIH) grant P30GM103392 (R. Friesel, PI), Phase III COBRE in Vascular Biology and the histopathology core facility supported by NIH grants P20GM103465/P30GM103392. Human heart tissue samples were obtained from the MMC BioBank, a core facility at Maine Medical Center Research Institute. LC-MS/MS analysis of sphingolipids was performed by Lipidomics Shared Resource, Medical University of South Carolina, MUSC. This work was conducted in a facility constructed with support from the National Institutes of Health, Grant Number C06 RR018823 from the Extramural Research Facilities Program of the National Center for Research Resources. The funders had no role in study design, data collection and analysis, decision to publish, or preparation of the manuscript.

Competing Interests: The authors have declared that no competing interests exist.

* E-mail: pinzi@mmc.org

Introduction

Lipotoxicity, the accumulation of lipids in non-adipose tissues due to increased plasma free fatty acids and triglycerides, has been well documented in type I and type II diabetes and in obesity [1–5]. The high incidence of hyperlipidemia in the U.S. population (30% of adults and unknown but growing numbers of children and adolescents) and its associated health challenges (coronary artery disease, hypertension, diabetes, heart failure, and stroke) make it imperative to understand the lipotoxic mechanisms that induce pathologic changes in tissues and organs. In particular, changes in cellular membrane lipid composition due to intracellular accumulation of lipids may have profound effects on membrane and organelle function. Several genetic rodent models recapitulate lipid accumulation in the heart, which is linked to lipid-induced cardiomyopathy [6–10].

To define the role of fatty acids in this process, previous studies have focused on the difference between the effects of saturated and unsaturated fatty acids on cardiac substrate utilization and the

contractile performance of isolated cardiomyocytes [11,12]. These studies show that exposing isolated cardiomyocytes to high concentrations of the saturated fatty acid palmitate induces contractile dysfunction and apoptosis [11,13–15]. In contrast to these studies, we have focused on the effect of palmitate on the caveolae membrane system.

Caveolae are plasma membrane invaginations, 50–100 nm in diameter, rich in cholesterol and sphingolipids [16], and are important in endocytosis, lipid trafficking, and signal transduction [17,18]. Originally discovered in the endothelium [19], caveolae have now been identified in many cell types including epithelium, adipocytes, fibroblasts, and smooth, skeletal, and cardiac muscle cells. Three caveolin proteins have been described: caveolin-1, caveolin-2, and caveolin-3. Caveolin-1 is ubiquitously expressed and is required for the formation of caveolae, while caveolin-3 is a muscle-specific caveolin that is predominantly expressed in skeletal and cardiac muscle. Caveolin-3 localizes not only to the plasma membrane but also to T-tubules and is essential for normal formation of the T-tubule system in the developing muscle and

heart [20,21]. Consequently, the loss of caveolin-3 in the mouse reduces the number of caveolae in muscle and induces T-tubule abnormalities and produces a phenotype similar to muscular dystrophy [22,23]. Loss of caveolin-1 or caveolin-3 in the heart induces hypertrophy that leads to dilated cardiomyopathy [24–27]. Caveolin-3 potentially also has an important role in cardiac calcium regulation [28,29]. Therefore, we tested the hypothesis that dietary palmitate intake, via accumulation of membrane sphingolipids, induces the loss of caveolin-3 and causes cardiac contractile dysfunction. We also tested whether the dietary induced loss of caveolin-3 is reversible by normalizing the dietary intake of fat.

Materials and Methods

Human left ventricular tissue

Embedded tissue blocks of autopsy material for a total of 5 non-obese normal, 4 obese with no cardiomyopathy, 9 obese with cardiomyopathy, and 7 non-obese with cardiomyopathy cases with non-identifying information were obtained from the Maine Medical Center BioBank and underwent immunohistochemistry staining for caveolin-3 in the histology core of MMCRI. Patients with a body mass index of >30 were considered obese. Exemption for inclusion of these tissue samples in this study was obtained from the IRB at MMCRI.

Animals

C57BL/6 mice of both genders were used. The age range covered by this study was 15–16 weeks for the 12-week feeding time point and 27–28 weeks for the 24-week time point. The Maine Medical Center Institutional Animal Care and Use Committee approved all experimental protocols. The handling and housing of mice followed the recommendations of current NIH and American Physiological Society guidelines for the care and use of laboratory animals.

Diet composition and feeding regimen

High lipid diets were custom made by Harlan Laboratories. All high fat diets contained 200 g/kg as fat (20%). In the high palmitate diet 90 g/kg was palmitate, equivalent to 41% of all fat being palmitate (Harlan TD05235) and fed ad libitum. The rationale for choosing this lipid composition is based on the average saturated fat content of a fast food meal and taking into consideration that the saturated fat content of hamburgers can be more than 30%. As control for the high fat content a diet was composed using medium chain triglycerides with the same caloric intake from fat as the high palmitate diet (Harlan TD05237). Standard laboratory chow was used as comparison with a crude fat content of 6%. Mice were changed to high fat diets at the age of 3–4 weeks and maintained for 12 weeks. After 12 weeks they underwent cardiac function assessment and a subset of mice were returned to normal standard laboratory chow for another 12 weeks. At the end of contractile function assessment, tissues were frozen and used for either total lipid analysis or caveolin protein determination. A subset of mice was used for isolating cardiomyocytes to determine intracellular localization of caveolin isoforms by confocal microscopy.

Blood plasma biochemistry

Blood plasma samples were obtained biweekly by cheek pouch bleeding. Glucose, ketones, cholesterol, HDL, and triglycerides levels in whole blood were determined using a CardioChek Analyzer (Polymer Technology Systems, Inc. Indianapolis, IN).

Insulin levels were measured using the ultrasensitive ELISA kit from ALPCO Diagnostics, Salem, NH.

Langendorff perfusion

Mice were anesthetized using avertin and the heart perfused following Pinz et al. [30]. Briefly: After cervical dislocation, the heart was quickly excised and arrested in ice-cold Krebs Henseleit buffer (in mM: EDTA 0.5, NaCl 118, KCl 5.3, Mg₂SO₄ 1.2, NaHCO₃ 25, CaCl₂ 2.5, glucose 10, pyruvate 0.5). Then, the heart was hung by the aorta to a cannula and perfused at a constant pressure of 75 mmHg. A water-filled balloon was inserted into the left ventricle via the left atrium and, by inflation, the end diastolic pressure was adjusted to 5–10 mmHg. The balloon line was connected to a pressure transducer and pressure changes in the left ventricle were followed on line with a PowerLab data acquisition system. To exclude differences in contractile performance due to varying heart rates, hearts were paced at 420 bpm throughout the protocol. Contractile performance was assessed in the presence of different extra-cellular calcium concentrations (1.5–4.0 mM) to determine contractile reserve with increasing cardiac workload and to define cardiac calcium sensitivity.

Isolation of adult mouse cardiomyocytes

Adult mouse cardiomyocytes were isolated following Pinz et al. [31]. Briefly, mouse hearts were perfused on a gravity flow system with Tyrode's solution containing calcium to clear coronaries of blood. Then calcium-free Tyrode's solution was used to initiate the digestion protocol. The enzymatic digestion of heart tissue was accomplished by using Liberase TH (Roche). Liberase TH solution was flushed from the heart tissue after 4–5 minutes with calcium-free Tyrode's solution, and then cardiomyocytes were mechanically dispersed by gently teasing apart tissue. Cells were re-adjusted to 1.2 mM extracellular calcium and were plated on mouse laminin coated cover slips. Only freshly isolated cells were used and cells were fixed the same day.

Confocal microscopy

After adhesion to laminin coated cover slips, cardiomyocytes were washed twice in ice cold PBS and fixed with 4% paraformaldehyde in PBS for 10 minutes at RT. Coverslips were washed with ice cold PBS and stored in PBS with 0.01% sodium azide. Fixed cells were blocked and permeabilized with 5% BSA, 0.1% Triton-X-100, 0.1% Tween20, and 0.1% sodium azide in PBS for 1 hour at RT. Primary antibodies were diluted in PBS with 1% BSA and 0.3% Triton-X-100: Caveolin-1 (Cell Signaling #3267, 1:200), Caveolin-3 (BD Transduction #610420, 1:300). Primary antibodies were incubated at 4°C overnight prior to conjugation with fluorescently labeled secondary antibodies. Alexa Fluor 488 labeled goat anti-mouse IgG 1:2000 (Invitrogen) and Alexa Fluor 546 goat anti-mouse IgG 1:2000 (Invitrogen) were incubated for 2 hours at RT. Counter staining with a DNA stain TOPRO (Invitrogen T3605, 1:1000) was completed for 30 minutes at RT directly after secondary antibody incubation. Cells were mounted with ProLong Gold anti-fade reagent (Invitrogen), allowed to cure overnight at RT, sealed and examined with a Leica TCS SP II True Confocal Laser Scanning Microscope and analyzed using the Leica confocal software.

Lipid extraction, fractionation, and mass spectrometry

ESI/MS/MS analysis of endogenous sphingosine bases, sphingoid base-1-phosphates, ceramide, and of endogenous sphingomyelin molecular species were performed on a Thermo-Fisher TSQ Quantum triple quadrupole mass spectrometer, operating in

a Multiple Reaction Monitoring (MRM) positive ionization mode, using modified version [32]. Briefly, for ceramide species, cardiac tissue extracts corresponding to 1 mg protein, were fortified with the internal standards (ISs: C₁₇ base D-erythro-sphingosine (17CSph), C₁₇ sphingosine-1-phosphate (17CSph-1P), N-palmitoyl-D-erythro-C₁₃ sphingosine (13C16-Cer) and heptadecanoyl-D-erythro-sphingosine (C17-Cer)), and extracted with ethyl acetate/isopropanol/water (60/30/10 v/v) solvent system. After evaporation and reconstitution in 100 µl of methanol samples were injected on the HP1100/TSQ Quantum LC/MS system and gradient eluted from the BDS Hypersil C8, 150×3.2 mm, 3 µm particle size column, with 1.0 mM methanol ammonium formate/2 mM aqueous ammonium formate mobile phase system. Peaks corresponding to the target analytes and internal standards were collected and processed using the Xcalibur software system. For sphingolipids, cardiac tissue extracts (1 mg protein), were fortified with the internal standards (IS): N-hexanoyl-1-(2-phosphorylcholine)-sphingosine (C6-SM), N-heptadecanoyl-1-(2-phosphorylcholine)-sphingosine (C17-SM) and extracted with ethyl acetate/isopropanol/water (60/30/10%v/v) solvent system. After evaporation and reconstitution in 1 ml of methanol 10 µl of 1M NaOH in methanol was added, then left for 2 hours at room temperature, and then subjected to Bligh & Dyer extraction (methanol/chloroform/water). The lower, organic phase was recovered, evaporated to dryness, and reconstituted in 200 µl of methanol. The reconstituted samples (10 µl) were injected into the LC/MS and analyzed as described above. Quantitative analysis for ceramide and sphingomyelin species was based on the calibration curves generated by introducing an artificial matrix with the known amounts of target analyte synthetic standards and an equal amount of the internal standards (ISs). The target analyte/IS peak areas ratios were plotted against analyte concentration. The target analyte/IS peak area ratios from the samples were similarly normalized to their respective ISs and compared to the calibration curves, using a linear regression model.

Statistics

Sphingolipid metabolites were analyzed with two-way ANOVA and Bonferroni post-hoc test, cardiac contractile function data were analyzed with linear regression analysis in GraphPad Prism (Prism 4, GraphPad Software, Inc.). All other data were analyzed with one-way ANOVA and p<0.05 was considered significant. Data are represented as mean ± SE.

Results

General characteristics of mice fed high fat diets

C57BL/6 mice (both genders) were maintained on standard, MCT or palmitate diet starting at 3 weeks of age for 12 weeks. To follow the change in blood lipid, glucose and insulin levels, blood samples were taken every two weeks. Over the time frame of this study there were no changes in blood parameters measured at any time points between diets: (all in mM, glucose: 5.8±0.8 standard, 5.4±0.4 MCT, 6.9±0.5 palmitate; ketones: 0.4±0.05 standard, 0.5±0.04 MCT, 0.5±0.02 palmitate; cholesterol: <2.59±0 standard, 3.6±0.1 MCT, 3.8±0.3 palmitate; HDL: 1.0±0.3 standard, <0.57±0 MCT, <0.57±0 palmitate; triglycerides: 1.0±0.3 standard, <0.57±0 MCT, <0.57±0 palmitate; n=9). The only exception were insulin levels, which increased after 10 weeks in mice maintained on the palmitate diet, which reached significance only at the 12-week time point: (insulin (nM): 0.3±0.004 standard, 0.4±0.05 MCT, 1.9±0.3* palmitate; n=6, * p<0.05, one-way ANOVA, Student Newman Keul’s posthoc comparison.). On the high fat control diet insulin levels remained

normal. Thus, mice remained normoglycemic and normolipidemic on either high fat diet, but were slightly hyperinsulinemic on the high palmitate diet for the duration of ~2 weeks before the endpoint of the study.

To determine whether feeding a high palmitate diet induces hypertrophic changes in the heart, mice were weighed weekly and heart and left ventricular (LV) weight were determined after 12 weeks (Table 1). Mice maintained on the palmitate diet gained slightly more body weight, however, no significant differences were observed between diets (Table 1). Balloon volumes, which are a measure of LV volume, were unchanged in all groups. Thus, there is no indication of morphological changes, such as hypertrophy, associated with the high fat diets chosen for this study.

Palmitate-induced ceramide and sphingomyelin accumulation in cardiac tissue

Ceramide and sphingomyelin species were determined in total lipid extracts of cardiac tissue after 12 weeks on the diets. Total ceramide levels (calculated as the sum of ceramide species) were significantly increased in palmitate diet fed mice with 393±19.4 pmol/mg protein (p=0.03 vs. standard diet, one-way ANOVA) compared to 129±6.3 pmol/mg protein and 295±14.3 pmol/mg protein in standard or control diet fed mice. Palmitate feeding preferentially caused the accumulation of medium- and long chain (C16, C20 and C20:1) ceramide species (Fig. 1A). Interestingly C18 did not increase, which is the ceramide species generated from de-novo synthesis from palmitate. This may suggest that there is an immediate deacetylation of C18 to C16 or an immediate acetylation to C20. The long chain ceramides from C22 to C24 did not show significant differences between standard, MCT or high palmitate diets. Other ceramide species were determined but data are not shown because of the low levels present.

The palmitate-induced accumulation of sphingomyelin did not reach significance for total sphingomyelin with 2170±308 pmol/mg protein in standard, 2284±401 pmol/mg protein in MCT, and 2837±71 pmol/mg protein in palmitate diet fed mice. However, there were significant changes in the accumulation of medium- and long chain length species, C16 and C20, between palmitate and standard or MCT diet fed mice (Fig. 1B). This result suggests that sphingomyelin synthase may limit the accumulation of medium chain ceramides by increasing the membrane content of medium chain sphingomyelins. Long chain sphingomyelins, C24 and C24:1, were significantly increased in the two high fat diets compared to standard diet.

These changes in sphingolipid levels cannot be achieved using synthetic ceramide or sphingomyelin species as only short chain

Table 1. General characteristics of mice at 12 weeks of the feeding regimen.

	standard	MCT	palmitate
n	5 (3m,2f)	7 (3m,4f)	5 (3m, 2 f)
BW (g)	27.2±4.7	25.9±4.1	30.7±6.1
LV (mg)	91±13.7	77±17	92±3.7
Bal vol. (µl)	12.3±4	10.4±3.7	9.4±2.2
HW (mg)	117±16	101±19	119±6
HW/BW (mg/g)	4.2±0.2	4.8±0.3	4.0±0.7

BW: body weight, HW: heart weight, Bal Vol.: balloon volume = left ventricular volume, LV: left ventricle, m: male, f: female. Means ± SE, n=5–7.
doi:10.1371/journal.pone.0061369.t001

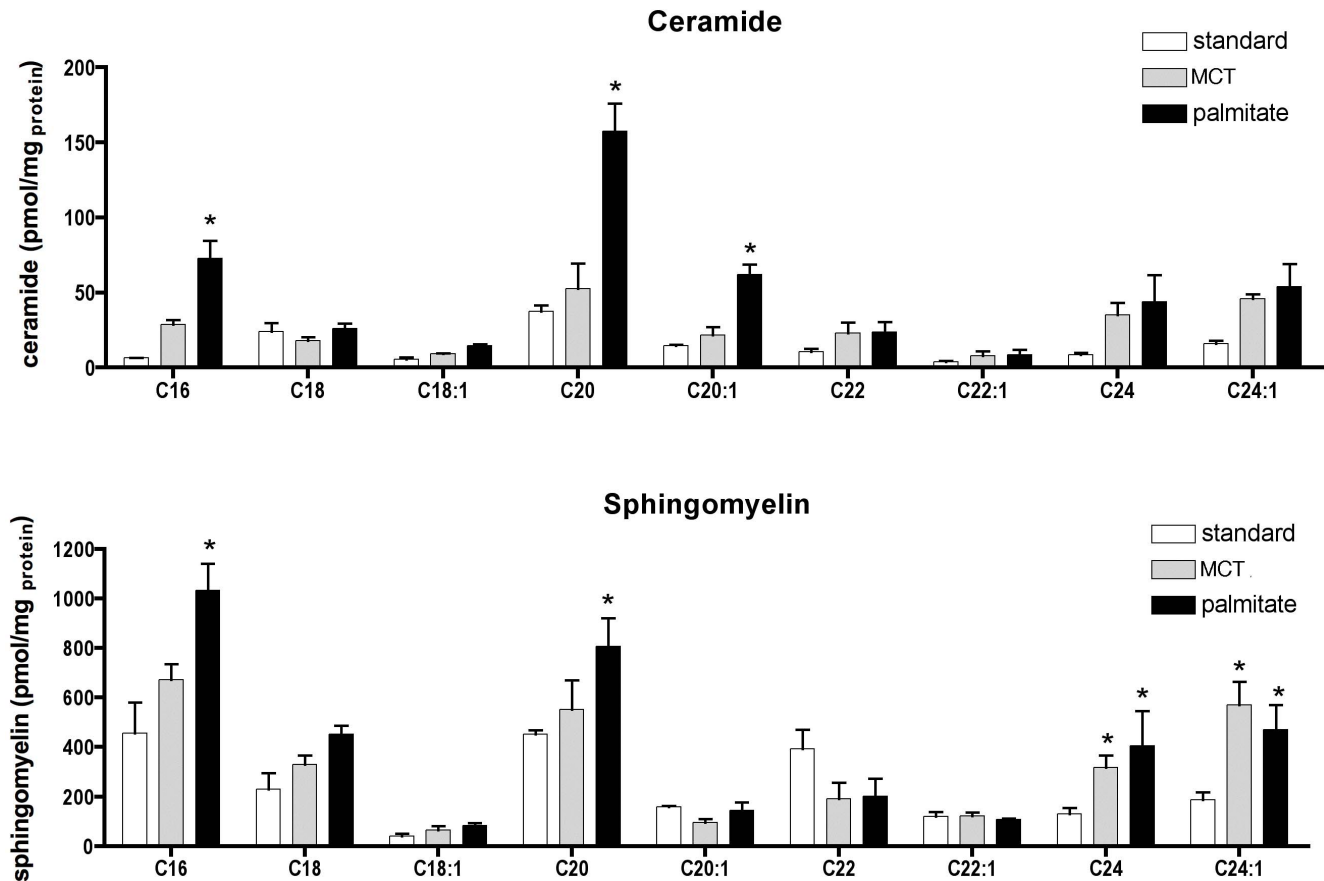


Figure 1. Palmitate increases medium and long chain ceramide and sphingomyelin species in left ventricular tissue. A) Levels of different ceramide species in total lipid extracts of left ventricular tissue determined by mass spectrometry after 12 weeks on standard, control or palmitate diet. Medium chain ceramides with C16, C20 and C20:1 increase in mice fed palmitate for 12 weeks. Long chain ceramides C24 and C24:1 are equally increased in control and palmitate diet fed mice, however these data did not reach significance. Mean \pm SE, $n=3$, two-way ANOVA, Bonferroni post-hoc analysis, * $p<0.05$. B) Sphingomyelin species levels at the 12 week feeding time point. Palmitate feeding led to an increase of medium chain sphingomyelin species C16 and C20. The long chain sphingomyelins, C24 and C24:1, are equally increased in mice fed control or palmitate diet compared with standard diet fed mice. Mean \pm SE, $n=3$ (2 male, 1female each group), two-way ANOVA, Bonferroni post-hoc analysis, * $p<0.05$. doi:10.1371/journal.pone.0061369.g001

species (C2–C6) reliably cross the plasma membrane. Short chain ceramides and sphingomyelins do not occur at physiological levels but have been used to investigate the mechanism of ceramide-induced apoptosis in cell culture [33].

Palmitate-induced systolic dysfunction after 12 weeks

Hearts of mice fed standard or MCT control diets had normal contractile performance, as indicated by the essentially equivalent calcium response curves at the 2, 4, and 12-week intervals (Fig. 2A–C). In contrast, after 12 weeks on the palmitate diet, mouse hearts showed systolic contractile dysfunction. Fig. 2A shows a 30% reduction in rate pressure product (RPP, a measure of the contractile work the heart performs) in high-palmitate-fed mice at 12 weeks. Positive dP/dt , the first derivative of pressure loss, a measure of contractility, showed a 40% reduction at 12 weeks (Fig. 2B). Maximum systolic pressure and developed pressure were similarly affected (data not shown). The contractile dysfunction was especially apparent at higher extracellular calcium concentrations, suggesting diminished calcium handling ability in these hearts. The diminished positive dP/dt indicates a slower release of calcium from the SR, which suggests that either the dihydropyridine receptor (DHPR, L-type calcium channel) or the ryanodine

receptor (RyR) or both are affected. The DHPR localizes to caveolae, and the extradiadic RyR is in close proximity to caveolae [29].

The sarcoendoplasmic reticulum calcium ATPase (SERCA2a) is a major calcium handling protein, and changes in its activity and expression levels are known to cause contractile dysfunction in heart failure [34]. We tested whether SERCA2A or DHPR levels were changed due to the palmitate diet. However, protein levels for both proteins were the same in all diets (Fig. 3) and data did not show a trend for diminished expression under any treatment conditions.

Palmitate-induced loss of T-tubular caveolin-3 and loss of striated RyR appearance

To further investigate the mechanism of palmitate-induced contractile dysfunction, we isolated cardiomyocytes from all groups of mice and determined the intracellular localization of caveolin proteins and their expression levels. Caveolin-1 and caveolin-3 are expressed in cardiomyocytes of standard diet fed mice and co-localize to the plasma membrane and the T-tubule system (Fig. 4A). The MCT control diet decreased caveolin-1 protein levels and some signal was observed in the nuclei. The

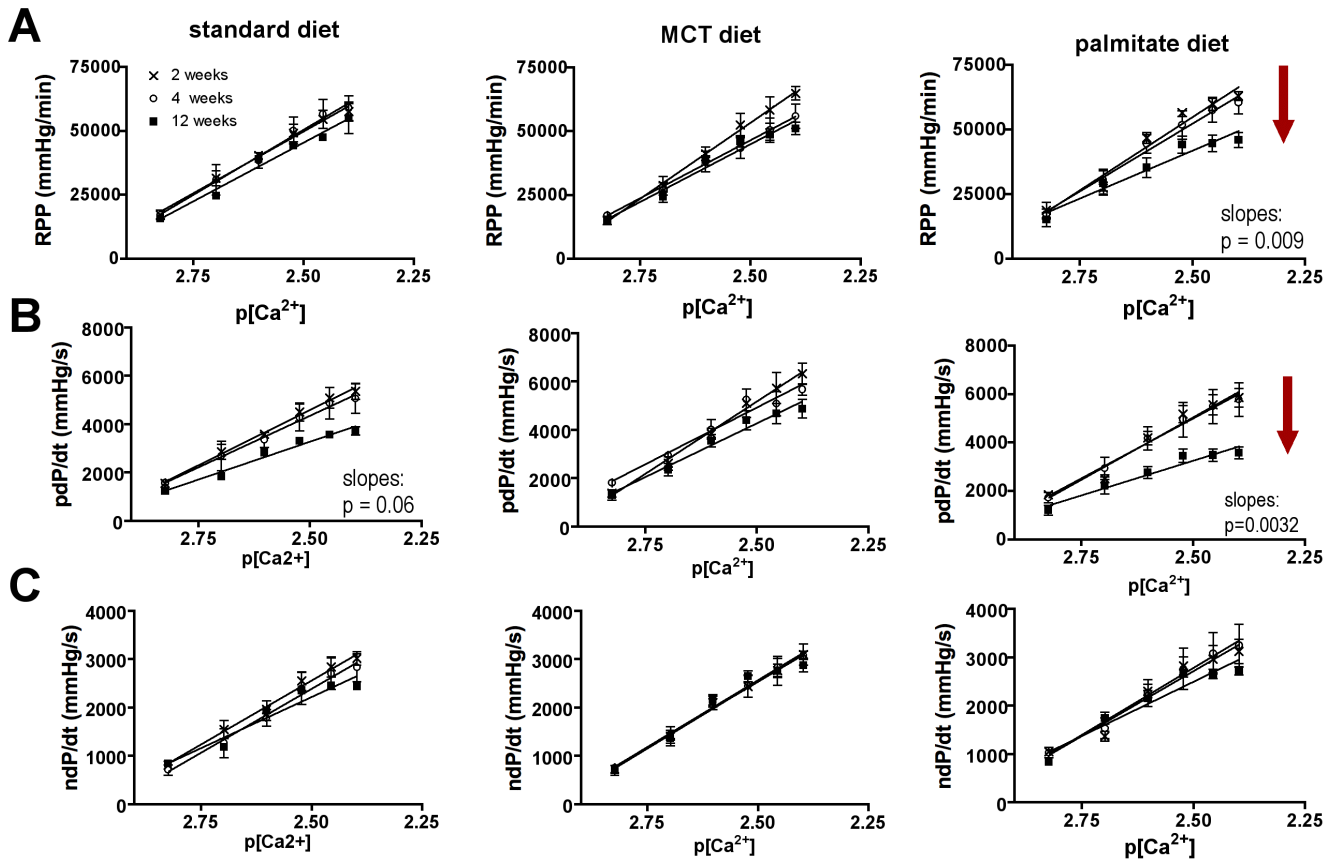


Figure 2. Palmitate diet causes systolic dysfunction in 12 weeks. **A**) Rate pressure product (RPP) vs. $p[Ca^{2+}]$ relationship for mouse hearts at 2 (x), 4 (○), and 12 (■) weeks of standard, MCT, and palmitate diet. RPP decreased by 30% in mice after 12 weeks on the palmitate diet. Means \pm SE, $n=4-8$, linear regression analysis through single data points using GraphPad Prism 4. **B**) pdP/dt vs. $p[Ca^{2+}]$ relationship of mice fed standard, MCT, and palmitate diet for 2, 4, or 12 weeks. pdP/dt is decreased by 40% in mice fed palmitate diet for 12 weeks. Means \pm SE, $n=4-8$, linear regression analysis through single data points using GraphPad Prism 4. **C**) ndP/dt vs. $p[Ca^{2+}]$ relationship for all diets over 2, 4 and 12 weeks. No differences were observed in diastolic contractile performance. Means \pm SE, $n=4-8$ (50/50 gender split in all groups), linear regression analysis through single data points using GraphPad Prism 4.
doi:10.1371/journal.pone.0061369.g002

observation that caveolin-1 can localize to the nucleus under these conditions is surprising, and it remains an open question whether this state represents a distinct signaling function. Caveolin-3 levels and intracellular localization did not change with MCT diet

feeding (Fig. 4A and B). In contrast, with high palmitate feeding, caveolin-3 is lost from the T-tubule system and from the plasma membrane, though diminished protein staining remains localized to the plasma membrane (Fig 4A). The expression of caveolin-3

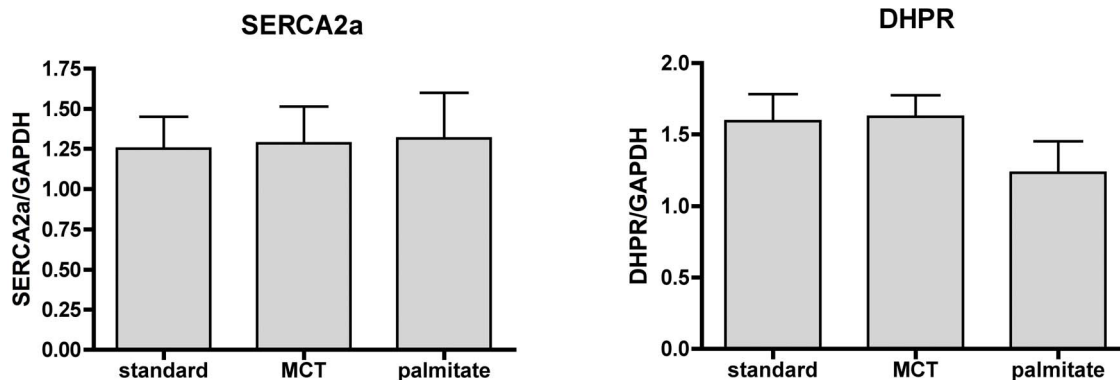


Figure 3. Palmitate diet does not change SERCA2a or DHPR protein levels. Quantification of SERCA (**A**) and DHPR (**B**) protein levels in LV tissue from hearts at the 12-week feeding time point. Protein levels were normalized to GAPDH levels. Both proteins are unchanged by the high fat feeding regimen. Means \pm SE, $n=6-9$ (3male and 3 female for $n=6$, or 5 male and 4 female for $n=9$).
doi:10.1371/journal.pone.0061369.g003

decreases by 90% compared to standard diet-fed mice (Fig. 4 A–C). In addition, there was a modest increase in caveolin-1 expression during palmitate feeding with unchanged intracellular localization (Fig. 4C). To support our findings with confocal microscopy, left ventricular tissue sections underwent immunohistochemistry and were stained for caveolin-3. Figure 4D shows that tissue of standard diet fed mice show caveolin-3 staining at the plasma membrane and the T-tubule systems, tissue of MCT diet fed mice has slightly lower overall staining, but caveolin-3 is observed at plasma membranes and the T-tubule system. In contrast, tissue of palmitate diet fed mice has low overall staining and some cardiomyocytes do not show any caveolin-3 protein at the plasma membrane or the T-tubule system. To further investigate the palmitate-induced changes in the intracellular localization of caveolin-3 we exposed HL-1 cardiomyocytes to increasing concentrations of palmitate (Fig. 4E). Cellular membrane systems were separated by sucrose gradient centrifugation and fractions were tested for the presence of caveolin-3 by western blotting. The higher the *in vitro* palmitate concentration was, the more caveolin-3 moved out of the high buoyant fraction (fraction 4, the so called caveolae fraction) to the low buoyant fractions (fractions 8–10), which consist of SR, ER and nuclear membranes.

The loss of caveolin-3 from the T-tubular system suggests a defect in this important membrane signaling system in the heart. Consistent with this idea, caveolin-3 null mice show defects in T-tubule development [35]. Therefore, to test whether palmitate-induced loss of caveolin-3 changes the T-tubule system in the heart, we used isolated cardiomyocytes and stained for ryanodine receptor to visualize the T-tubule system. Figure 5 shows that in standard diet and MCT diet fed mice the T-tubule system is depicted by RyR staining. However, in palmitate diet fed mice there is less RyR staining and in some areas a complete loss of staining. Thus, the diminished contractile performance in the presence of higher extracellular calcium suggests that a defect in the T-tubule system likely coupled with lower RyR expression, which we base on the lower staining in confocal images, cause palmitate – induced contractile dysfunction.

The loss of caveolin-3 in palmitate diet fed mice is consistent with the loss of caveolin-3 in cardiac samples from obese humans (Fig. 6). Although the dietary preferences of these individuals are unknown, the fact that their body mass index was above 30 strongly suggests hyperlipidemia in these individuals. Also there is a clear distinction between cases with non-obese cardiomyopathy and obese cardiomyopathy in the amount of caveolin-3 present in the T-tubule system (white arrows). These data support our findings in mice and support the role of caveolin-3 in lipid induced contractile dysfunction.

Dietary intervention is sufficient to reverse palmitate-induced caveolin-3 loss

To find out whether the lipid-induced changes in cardiac membranes and the loss of caveolin-3 is reversible, we changed the high fat diet fed mice after 12 weeks to normal laboratory chow for another 12 weeks. Western blotting confirmed that caveolin-1 and caveolin-3 levels normalize (Fig. 7A) and contractile performance and calcium sensitivity in the isolated heart was also normal (Fig. 7B), showing no significant differences between standard, MCT, and palmitate diets at this time point.

Discussion

Obesity is a growing epidemic in the Western world and understanding mechanisms of the associated cardiovascular diseases is imperative for developing treatment strategies. Here

we present a new mechanism for lipid-induced cardiac contractile dysfunction that resembles the cardiomyopathy observed in caveolin-3 loss-of-function mice [25]. We present evidence that high intake of dietary palmitate disturbs sphingolipid homeostasis, which leads to contractile dysfunction by inducing the loss of caveolin-3 from the T-tubule membrane system. Our findings are further supported by immunohistochemistry findings in human cardiac tissue samples of non-obese and obese humans, in which the obese tissue samples showed a drastic reduction of caveolin-3 expression in cardiomyocytes.

Palmitate-induced contractile dysfunction is independent of mechanisms causing lipid-induced diabetic cardiomyopathy

Previous studies used high fat feeding to induce insulin resistance and diabetes. For example, Kim et al. [36] compared 10% and 60% fat content in rodent diets and found insulin resistance and diabetes after 8 weeks in mice fed the 60% fat diet. Similarly, Lessard et al. [37] used 58% fat content in rats to induce insulin resistance in 4 weeks. In contrast to these studies, the time line of this high-fat feeding study and the lipid content was chosen in such a way that mice were not insulin resistant or diabetic. After 12 weeks on either the MCT or the palmitate diet mice were not hyperglycemic, hypertriglyceridemic or hypercholesterolemic. Only the palmitate diet-fed group had slight hyperinsulinemia with an onset at 10 weeks of palmitate diet feeding. Thus, our work suggests that contractile dysfunction and diabetic cardiac changes are, under our conditions, independent and uncoupled events.

Sphingolipid accumulation disturbs calcium regulation and causes systolic contractile dysfunction

The exposure to palmitate and subsequent accumulation of ceramide has long been considered detrimental to tissues due to its activation of apoptotic effectors, including JNK [14], mitochondrial cytochrome C release [38], Bax expression [39], and caspase 3 activation. To further investigate the mechanism of ceramide on cells, many studies used synthetic short chain ceramides that are easily taken up by the cells and are subsequently metabolized. However, these short chain ceramides may change the biophysical properties of the membrane in a different way than long-chain ceramides do [40], as they cause less disturbances in the lipid bilayer formation. To overcome this concern, we used a different, more biologically relevant approach to increase cardiac tissue levels of ceramides and sphingomyelins. Feeding a palmitate rich diet led to the accumulation of medium and long-chain ceramides and sphingomyelins, which were incorporated into cellular membranes. Other studies have shown that palmitate exposure induces apoptosis in cardiomyocytes [14,41,42]. To determine whether our approach of dietary palmitate induces apoptosis, we tested for caspase-3 activation and performed TUNEL staining in histological sections of cardiac tissue. We did not observe activation of caspase-3 in the palmitate diet fed mice. More over, TUNEL staining of cardiac tissue was negative as well (data not shown). This result suggests that dietary delivery of palmitate is different from direct palmitate exposure *in vitro* and provides the advantage of not inducing apoptosis in the heart. Thus, we conclude that the contractile dysfunction we observed in the palmitate diet fed mice is primarily associated with the inability of the hearts to regulate calcium levels.

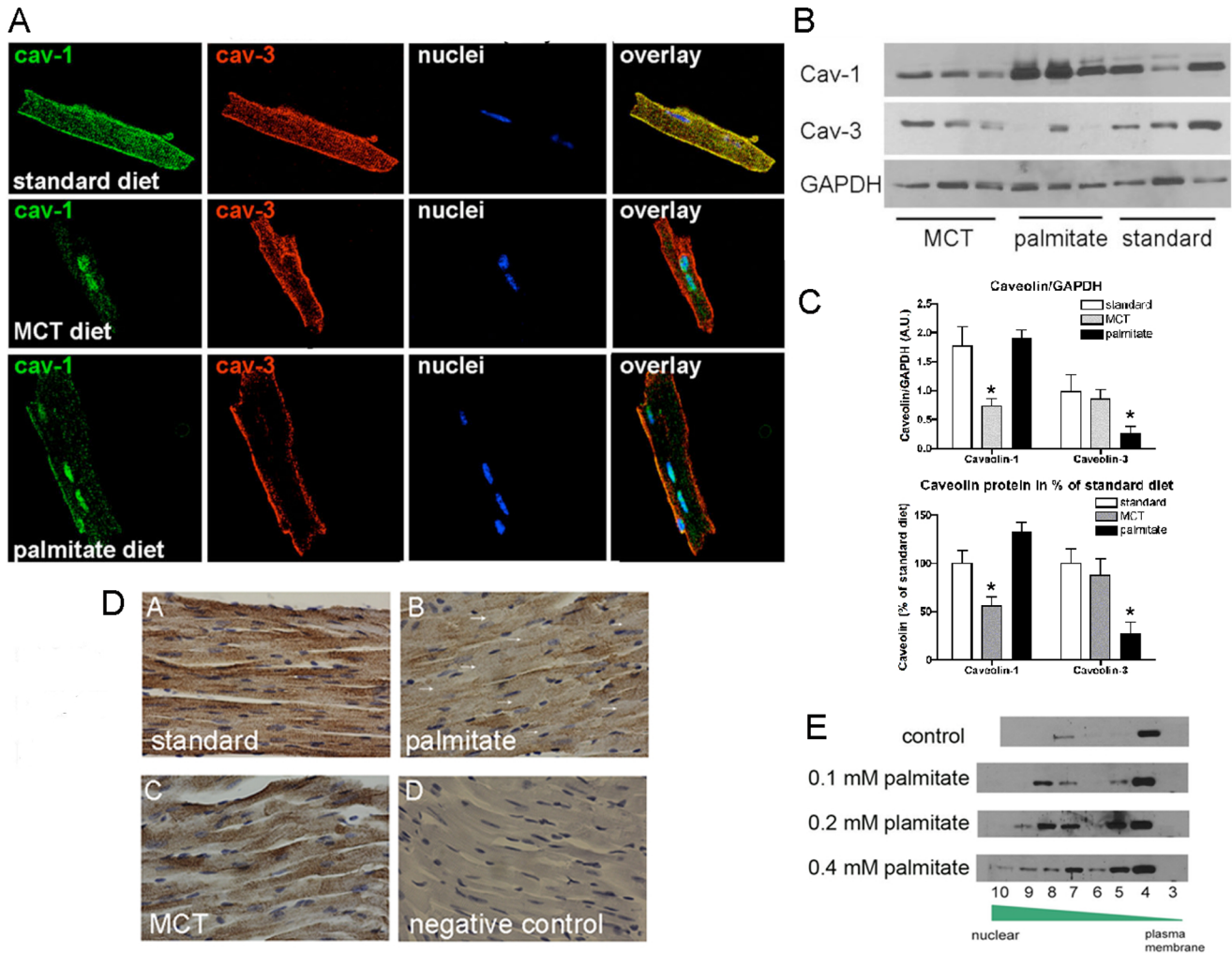


Figure 4. Palmitate-induced loss of caveolin-3 from the T-tubule system in the heart. **A)** Localization of caveolin-1 and -3 in confocal images of isolated cardiomyocytes from mice fed standard, MCT or palmitate diet for 12 weeks. Both caveolins co-localize in cardiomyocytes from standard diet fed mice, whereas caveolin-1 decreases in MCT diet fed mice and caveolin-3 is lost from the T-tubule system in palmitate diet fed mice. **B)** Western blot for caveolin-1 and -3 for all diets. **C)** Quantification of Western blots using GAPDH as loading control (top panel) and percent changes in the lower panel. N=5 (3 male, 2 female), * p<0.05 one-way ANOVA. **D)** Representative images of immunohistochemistry for caveolin-3 in left ventricular tissue sections of standard, MCT, and palmitate diet fed mice. Caveolin-3 staining is observed at the plasma membrane and the T-tubule system in standard diet fed mice. The overall signal intensity is modestly decreased in MCT diet fed mice, but caveolin-3 also localizes to the plasma membrane and the T-tubule system. In palmitate diet-fed mice there is significant loss of caveolin-3 staining. Some cardiomyocytes do not show any staining for caveolin-3 (white arrows) at the plasma membrane or the T-tubules. N=4 per diet. **E)** Cellular membrane fractionations by sucrose gradient centrifugation. HL-1 cardiomyocytes were exposed to increasing concentrations of BSA-complexed palmitate (0.1, 0.2, and 0.4 mM) and then underwent sucrose gradient centrifugation to separate the different membrane systems of the cells. By convention fraction 4 is considered the high buoyant, caveolae fraction and with increasing fraction number, buoyancy decreases and membranes become denser. Exposure to palmitate causes caveolin-3 to move from the caveolae fraction (fraction 4) to the denser membrane fractions (fraction 8–10), which represent SR, ER, and nuclear membranes. Experiment repeated 4 times with similar results. doi:10.1371/journal.pone.0061369.g004

Palmitate-induced loss of membrane caveolin-3 as a new mechanism for lipid-induced cardiomyopathy

At least 30 inactivating mutations have been identified in the human gene coding for caveolin-3, that lead to the loss of caveolae in skeletal muscle with four major associated disease complexes: limb-girdle muscular dystrophy, rippling muscle disease, hyperCKemia, and distal myopathy [43–46]. These diseases are mainly autosomal-dominant, and patients present with a broad range of symptoms that overlap between the four diseases. In the heart, caveolin-3 mutations are associated with hypertrophic and dilated cardiomyopathy [47] and long-QT syndrome [48]. In

addition, caveolin-3 mutations seem important in some cases of sudden infant death syndrome [49]. All mutations result in decreased caveolin-3 and caveolae in muscle cells. The loss of caveolin-3 in the mouse reduces the number of caveolae in muscle and induces T-tubule abnormalities and a phenotype similar to muscular dystrophy [35]. Caveolin-3 null mice also develop cardiac hypertrophy that leads to dilated cardiomyopathy [25,50]. Our study shows that palmitate-induced loss of caveolin-3 is associated with a contractile dysfunction phenotype that is similar to the cardiomyopathy reported in the caveolin-3 null mice [35]. To determine the underlying defect in calcium regulation, we

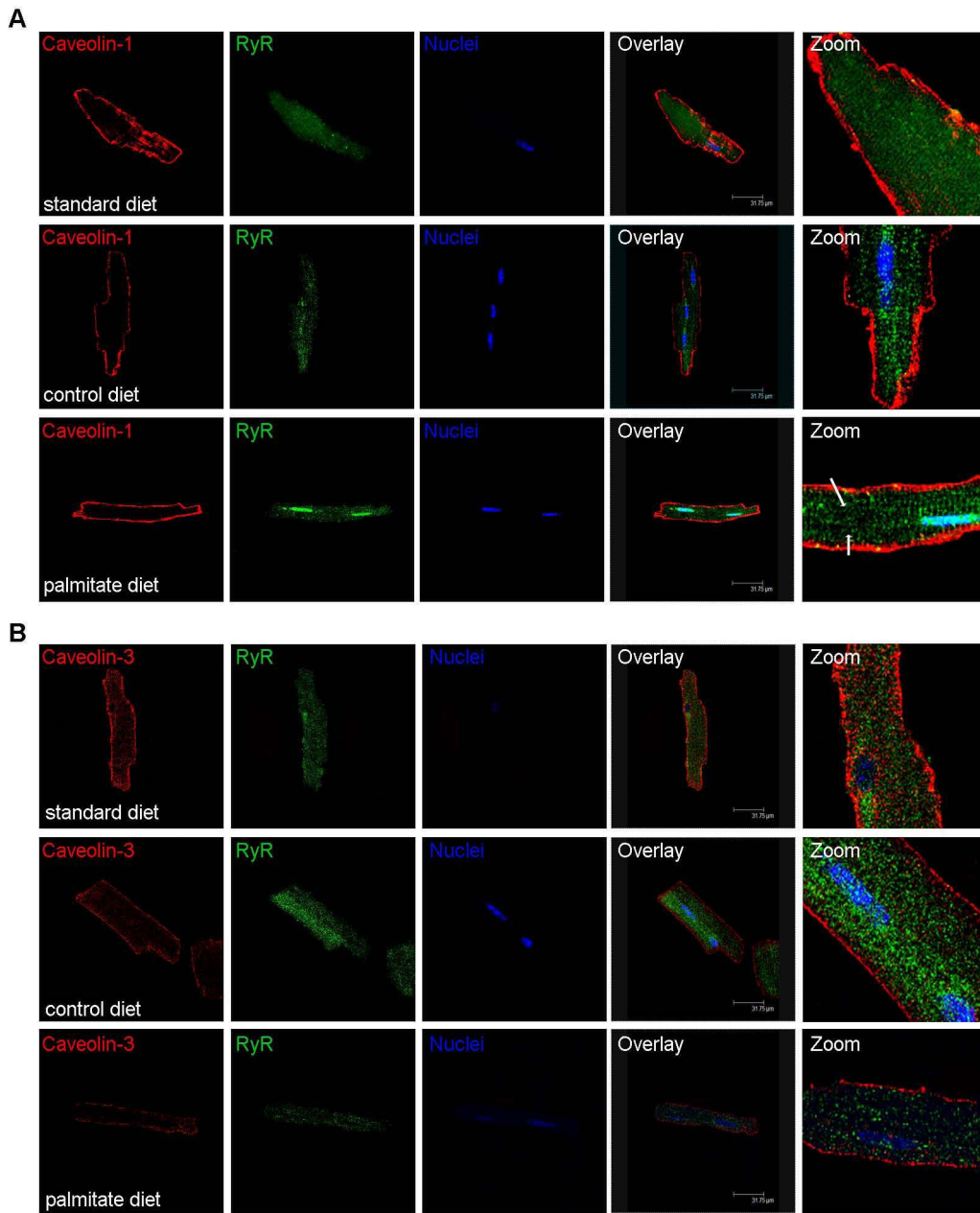


Figure 5. Palmitate-induced loss of T-tubular caveolin-3 and loss of striated appearance of the RyR localization. Intracellular localization of caveolin-1 (A) or caveolin-3 (B) and RyR in isolated cardiomyocytes from standard, MCT or palmitate diet fed mice. Caveolin-1 and -3 localize to the plasma membrane and the T-tubule system in standard diet fed mice (first row of panels in A and B). In MCT diet fed mice caveolin-1 expression decreases (second row of panels in A) but caveolin-3 expression remains unchanged (second row of panels in B). MCT diet does not change the striated appearance of the RyR (compare both middle panels in A and B). Palmitate diet does not change the expression or localization of caveolin-1 (third row panel A), but expression of caveolin-3 decreases and it is absent from the T-tubule system. In these areas the striated appearance of the RyR is lost (arrows in A and B). All confocal experiments were repeated at least 4 times with similar results. doi:10.1371/journal.pone.0061369.g005

determined expression of the most important calcium regulating proteins in the heart, SERCA, DHPR, and the ryanodine receptor. SERCA and DHPR levels were unchanged in hearts from palmitate diet-fed mice, consistent with an unchanged diastolic contractile function. In contrast to SERCA, the RyR was downregulated in cardiomyocytes from palmitate diet-fed mice (Fig. 5). The decrease and mislocalization of RyR protein is consistent with the loss of T-tubule structure, which is expected to

cause impaired calcium handling and contractile dysfunction. Recently, the direct binding of the dihydropyridine receptor and caveolin-3 was reported in skeletal muscle [51]. The dihydropyridine receptor is the partner of the RyR and responsible for the inflow of the trigger calcium that activates the RyR. We suggest that the loss of caveolin-3 disturbs the close interaction between the dihydropyridine receptor and the RyR, interfering with the calcium-induced calcium release. Importantly, we show

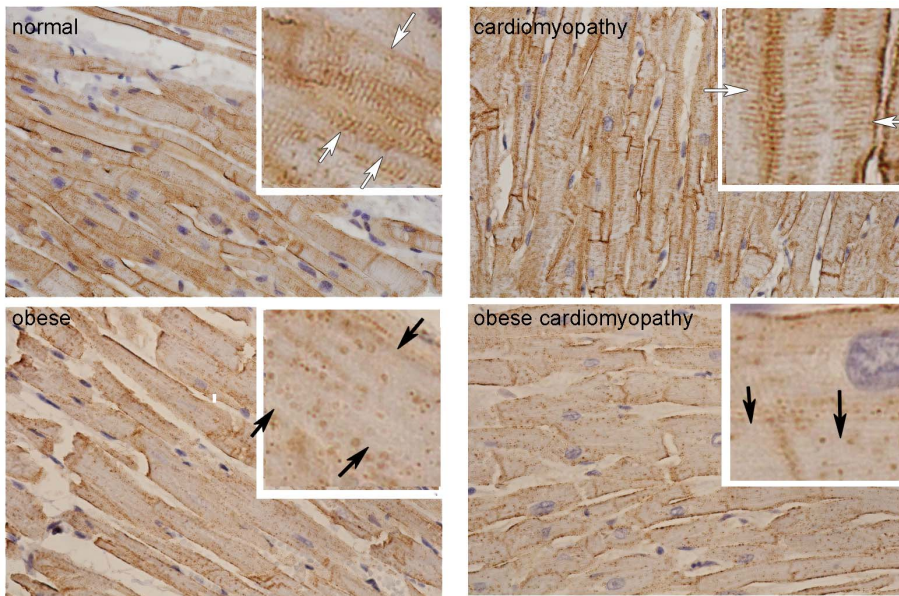


Figure 6. Caveolin-3 expression is decreased in obese human cardiac LV tissue. Representative immunohistochemistry showing caveolin-3 in normal, obese, obese with cardiomyopathy, and non-obese cardiomyopathy human left ventricular cardiac tissue. In normal human cardiomyocytes (upper left panel) caveolin-3 is expressed at the plasma membrane and the T-tubule system (white arrows). In obesity (lower left panel), the expression of caveolin-3 is drastically decreased in the T-tubule system (black arrows), which can occur independent of associated heart disease as the samples with cardiomyopathy (upper right panel) show, but seem to be enhanced in obese cases with cardiomyopathy (lower right panel).

doi:10.1371/journal.pone.0061369.g006

that dietary intervention is sufficient to reverse the palmitate-induced caveolin-3 loss. This reversibility indicates that caveolin-3 loss is regulated by dietary lipid intake, and that changes in membrane lipids can be reversed. This finding of reversibility has high translational significance, as simple dietary intervention may be sufficient to prevent and reverse the progression of the cardiomyopathic phenotype that develops in a subset of obese individuals.

Recently, the loss of T-tubule structure and organization was found to be a common theme for heart failure of different etiologies and in different species [52–55]. In particular, the work by Wei et al. [55] shows that the degree of heart failure is linked to the degree of T-tubule loss. The importance of this membrane system for cardiac contractile performance is further supported by the binding of beta adrenergic receptors to caveolins [56] and the

work by Nikolaev et al. [54] who showed that in heart failure beta2 adrenergic receptors, which are found in the T-tubule system, re-localize to plasma membrane areas essentially eliminating the distinction of beta1 and beta2 adrenergic responses in the failing heart. Based on these studies and the fact that caveolin-3 is required for normal T-tubule formation during cardiac development [20,35], because caveolin-3 is a crucial and important scaffolding protein that enables compartmentalization of cellular signaling, we suggest that the expression and intracellular localization of caveolin-3 in heart failure should be investigated as a potential therapeutic target for the improvement of contractile function. This view is further supported by the significant loss of caveolin-3 in heart samples of obese humans, which can be observed prior to other morphological changes that are associated with cardiomyopathy and heart failure.

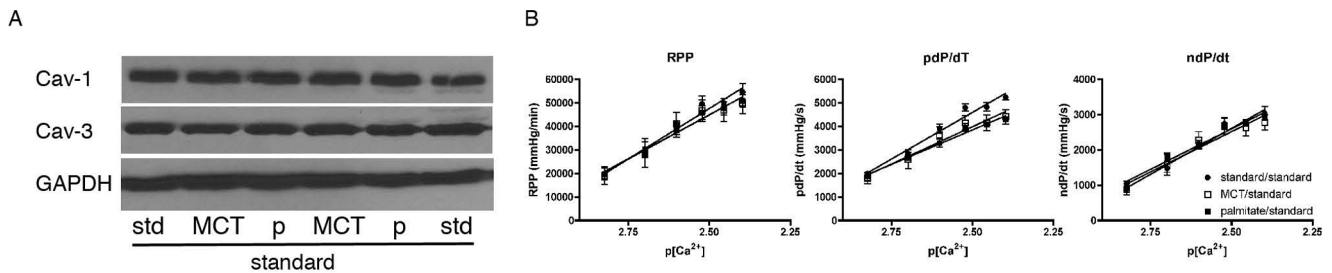


Figure 7. Dietary intervention is sufficient to reverse palmitate-induced caveolin-3 loss. **A)** Western blots of cardiac tissue of mice maintained on standard, MCT, or palmitate diet for 12 weeks followed by 12 weeks of standard laboratory chow feeding. Caveolin-1 and -3 expression is normal. (Std standard, MCT medium chain triglyceride high fat control diet, P palmitate). **B)** Ex vivo contractile performance (RPP, pdP/dt and ndP/dt) and calcium sensitivity normalizes after 12 weeks of standard laboratory chow feeding. N=6 (3 male and 3 female) per diet, linear regression analysis is not significant.

doi:10.1371/journal.pone.0061369.g007

Author Contributions

Conceived and designed the experiments: IMP CJK MC. Performed the experiments: IMP CJK MC. Analyzed the data: IMP CJK MC.

Contributed reagents/materials/analysis tools: IMP CJK MC. Wrote the paper: IMP CJK MC.

References

- Shankar SS, Steinberg HO (2005) FFAs: do they play a role in vascular disease in the insulin resistance syndrome? *Curr Diab Rep* 5: 30–35.
- Hallgren B, Stenhagen S, Svanborg A, Svennerholm L (1960) Gas chromatographic analysis of the fatty acid composition of the plasma lipids in normal and diabetic subjects. *J Clin Invest* 39: 1424–1434. doi:10.1172/JCI104162.
- Laakso M, Voutilainen E, Sarlund H, Aro A, Pyorala K, et al. (1985) Serum lipids and lipoproteins in middle-aged non-insulin-dependent diabetics. *Atherosclerosis* 56: 271–281.
- Zuniga-Guajardo S, Zimman B (1985) The metabolic response to the euglycemic insulin clamp in type I diabetes and normal humans. *Metabolism* 34: 926–930.
- Campbell PJ, Carlson MG, Nuijhan N (1994) Fat metabolism in human obesity. *Am J Physiol* 266: E600–E605.
- Chiu HC, Kovacs A, Ford DA, Hsu FF, Garcia R, et al. (2001) A novel mouse model of lipotoxic cardiomyopathy. *J Clin Invest* 107: 813–822.
- Chiu HC, Kovacs A, Blanton RM, Han X, Courtois M, et al. (2005) Transgenic expression of fatty acid transport protein 1 in the heart causes lipotoxic cardiomyopathy. *Circ Res* 96: 225–233.
- Yagyu H, Chen G, Yokoyama M, Hirata K, Augustus A, et al. (2003) Lipoprotein lipase (LpL) on the surface of cardiomyocytes increases lipid uptake and produces a cardiomyopathy. *J Clin Invest* 111: 419–426.
- Young ME, Guthrie PH, Razeghi P, Leighton B, Abbasi S, et al. (2002) Impaired long-chain fatty acid oxidation and contractile dysfunction in the obese Zucker rat heart. *Diabetes* 51: 2587–2595.
- Zhou YT, Grayburn P, Karim A, Shimabukuro M, Higa M, et al. (2000) Lipotoxic heart disease in obese rats: implications for human obesity. *Proc Natl Acad Sci USA* 97: 1784–1789.
- Fauconnier J, Andersson DC, Zhang SJ, Lanner JT, Wibom R, et al. (2007) Effects of palmitate on Ca(2+) handling in adult control and ob/ob cardiomyocytes: impact of mitochondrial reactive oxygen species. *Diabetes* 56: 1136–1142.
- Okere IC (2006) Differential effects of saturated and unsaturated fatty acid diets on cardiomyocyte apoptosis, adipose distribution, and serum leptin. *AJP: Heart and Circulatory Physiology* 291: H38–H44.
- Kong J (2003) Mitochondrial effects with ceramide-induced cardiac apoptosis are different from those of palmitate. *Archives of Biochemistry and Biophysics* 412: 196–206.
- Miller TA, LeBrasseur NK, Cote GM, Trucillo MP, Pimentel DR, et al. (2005) Oleate prevents palmitate-induced cytotoxic stress in cardiac myocytes. *Biochemical and Biophysical Research Communications* 336: 309–315.
- Tsang M (2004) Palmitate increases nitric oxide synthase activity that is involved in palmitate-induced cell death in cardiomyocytes. *Nitric Oxide* 10: 11–19.
- Stan RV (2005) Structure of caveolae. *Biochim Biophys Acta* 1746: 334–348.
- Anderson RG (1998) The caveolae membrane system. *Annu Rev Biochem* 67: 199–225.
- Okamoto T, Schlegel A, Scherer PE, Lisanti MP (1998) Caveolins, a family of scaffolding proteins for organizing “preassembled signaling complexes” at the plasma membrane. *J Biol Chem* 273: 5419–5422.
- Bruns RR, Palade GE (1968) Studies on blood capillaries. I. General organization of blood capillaries in muscle. *J Cell Biol* 37: 244–276.
- Parton RG, Way M, Zorzi N, Stang E (1997) Caveolin-3 associates with developing T-tubules during muscle differentiation. *The Journal of Cell Biology* 136: 137–154.
- Biederer CH (2000) The Basic Helix-Loop-Helix Transcription Factors Myogenin and Id2 Mediate Specific Induction of Caveolin-3 Gene Expression during Embryonic Development. *Journal of Biological Chemistry* 275: 26245–26251.
- Galbati F, Engelman JA, Volonte D, Zhang XL, Minetti C, et al. (2001) Caveolin-3 null mice show a loss of caveolae, changes in the microdomain distribution of the dystrophin-glycoprotein complex, and t-tubule abnormalities. *J Biol Chem* 276: 21425–21433.
- Smythe GM (2003) A caveolin-3 mutant that causes limb girdle muscular dystrophy type 1C disrupts Src localization and activity and induces apoptosis in skeletal myotubes. *Journal of Cell Science* 116: 4739–4749.
- Augustus AS, Buchanan J, Gutman E, Rengo G, Pestell RG, et al. (2008) Hearts lacking caveolin-1 develop hypertrophy with normal cardiac substrate metabolism. *Cell Cycle* 7: 2509–2518.
- Woodman SE, Park DS, Cohen AW, Cheung MW-C, Chandra M, et al. (2002) Caveolin-3 knock-out mice develop a progressive cardiomyopathy and show hyperactivation of the p42/44 MAPK cascade. *J Biol Chem* 277: 38988–38997.
- Park DS, Woodman SE, Schubert W, Cohen AW, Frank PG, et al. (2002) Caveolin-1/3 double-knockout mice are viable, but lack both muscle and non-muscle caveolae, and develop a severe cardiomyopathic phenotype. *Am J Pathol* 160: 2207–2217.
- Zhao Y-Y, Liu Y, Stan R-V, Fan L, Gu Y, et al. (2002) Defects in caveolin-1 cause dilated cardiomyopathy and pulmonary hypertension in knockout mice. *Proc Natl Acad Sci USA* 99: 11375–11380.
- Vassilopoulos S, Oddoux S, Groh S, Cacheux M, Fauré J, et al. (2010) Caveolin 3 Is Associated with the Calcium Release Complex and Is Modified via *In Vivo* Triadin Modification. *Biochemistry* 49: 6130–6135.
- Balijepalli RC, Foell JD, Hall DD, Hell JW, Kamp TJ (2006) Localization of cardiac L-type Ca(2+) channels to a caveolar macromolecular signaling complex is required for beta(2)-adrenergic regulation. *Proc Natl Acad Sci USA* 103: 7500–7505.
- Pinz I, Wax SD, Anderson P, Ingwall JS (2008) Low over-expression of TNFalpha in the mouse heart increases contractile performance via TNFR1. *J Cell Biochem* 105: 99–107.
- Pinz I, Zhu M, Mende U, Ingwall JS (2011) An Improved Isolation Procedure for Adult Mouse Cardiomyocytes. *Cell Biochem Biophys*.
- Bielawski J, Szulc ZM, Hannun YA, Bielawska A (2006) Simultaneous quantitative analysis of bioactive sphingolipids by high-performance liquid chromatography-tandem mass spectrometry. *Methods* 39: 82–91.
- Cremesti AE, Goni FM, Kolesnick R (2002) Role of sphingomyelinase and ceramide in modulating rafts: do biophysical properties determine biologic outcome? *FEBS Letters* 531: 47–53.
- Smith G (2007) Matters of the heart: the physiology of cardiac function and failure. *Experimental Physiology* 92: 973–986.
- Galbati F, Engelman JA, Volonte D, Zhang XL, Minetti C, et al. (2001) Caveolin-3 null mice show a loss of caveolae, changes in the microdomain distribution of the dystrophin-glycoprotein complex, and t-tubule abnormalities. *J Biol Chem* 276: 21425–21433.
- Kim F, Pham M, Luttrell I, Bannerman DD, Tupper J, et al. (2007) Toll-Like Receptor-4 Mediates Vascular Inflammation and Insulin Resistance in Diet-Induced Obesity. *Circulation Research* 100: 1589–1596.
- Lessard SJ, Rivas DA, Chen ZP, Bonen A, Febbraio MA, et al. (2007) Tissue-Specific Effects of Rosiglitazone and Exercise in the Treatment of Lipid-Induced Insulin Resistance. *Diabetes* 56: 1856–1864.
- Parra V, Eisner V, Chiong M, Criollo A, Moraga F, et al. (2007) Changes in mitochondrial dynamics during ceramide-induced cardiomyocyte early apoptosis. *Cardiovascular Research* 77: 387–397.
- Peterson JM, Wang Y, Bryner RW, Williamson DL, Alway SE (2008) Bax signaling regulates palmitate-mediated apoptosis in C2C12 myotubes. *Am J Physiol Endocrinol Metab* 295: E1307–E1314.
- Carrer DC, Schreier S, Patrio M, Maggio B (2006) Effects of a Short-Chain Ceramide on Bilayer Domain Formation, Thickness, and Chain Mobility: DMPG and Asymmetric Ceramide Mixtures. *Biophysical Journal* 90: 2394–2403.
- Kong JY, Rabkin SW (2004) Reduction of palmitate-induced cardiac apoptosis by fenofibrate. *Mol Cell Biochem* 258: 1–13.
- Zhu H, Yang Y, Wang Y, Li J, Schiller PW, et al. (2011) MicroRNA-195 promotes palmitate-induced apoptosis in cardiomyocytes by down-regulating Sirt1. *Cardiovascular Research* 92: 75–84.
- Minetti C, Sotgia F, Bruno C, Scartezzini P, Broda P, et al. (1998) Mutations in the caveolin-3 gene cause autosomal dominant limb-girdle muscular dystrophy. *Nat Genet* 18: 365–368.
- Hnasko R, Lisanti MP (2003) The biology of caveolae: lessons from caveolin knockout mice and implications for human disease. *Mol Interv* 3: 445–464.
- Sotgia F, Woodman SE, Bonuccelli G, Capozza F, Minetti C, et al. (2003) Phenotypic behavior of caveolin-3 R26Q, a mutant associated with hyperCK-emia, distal myopathy, and rippling muscle disease. *Am J Physiol Cell Physiol* 285: C1150–C1160.
- Woodman SE, Sotgia F, Galbati F, Minetti C, Lisanti MP (2004) Caveolinopathies: mutations in caveolin-3 cause four distinct autosomal dominant muscle diseases. *Neurology* 62: 538–543.
- Hayashi T, Arimura T, Ueda K, Shibata H, Hohda S, et al. (2004) Identification and functional analysis of a caveolin-3 mutation associated with familial hypertrophic cardiomyopathy. *Biochemical and Biophysical Research Communications* 313: 178–184.
- Rajab A, Straub V, McCann IJ, Seelow D, Varon R, et al. (2010) Fatal Cardiac Arrhythmia and Long-QT Syndrome in a New Form of Congenital Generalized Lipodystrophy with Muscle Rippling (CGL4) Due to PTRF-CAVIN Mutations. *PLoS Genet* 6: e1000874.
- Cronk LB, Ye B, Kaku T, Tester DJ, Vatta M, et al. (2007) Novel mechanism for sudden infant death syndrome: persistent late sodium current secondary to mutations in caveolin-3. *Heart Rhythm* 4: 161–166.
- Park DS, Woodman SE, Schubert W, Cohen AW, Frank PG, et al. (2002) Caveolin-1/3 double-knockout mice are viable, but lack both muscle and non-muscle caveolae, and develop a severe cardiomyopathic phenotype. *Am J Pathol* 160: 2207–2217.
- Couchoux H, Bichraoui H, Chouabe C, Altafaj X, Bonvallet R, et al. (2011) Caveolin-3 is a direct molecular partner of the Cav1.1 subunit of the skeletal muscle L-type calcium channel. *Int J Biochem Cell Biol* 43: 713–720.

52. Lyon AR, MacLeod KT, Zhang Y, Garcia E, Kanda GK, et al. (2009) Loss of T-tubules and other changes to surface topography in ventricular myocytes from failing human and rat heart. *Proc Natl Acad Sci USA* 106: 6854–6859.
53. Louch W (2004) Reduced synchrony of Ca²⁺ release with loss of T-tubules—a comparison to Ca²⁺ release in human failing cardiomyocytes. *Cardiovascular Research* 62: 63–73.
54. Nikolaev VO, Moshkov A, Lyon AR, Miragoli M, Novak P, et al. (2010) 2-Adrenergic Receptor Redistribution in Heart Failure Changes cAMP Compartmentation. *Science* 327: 1653–1657.
55. Wei S, Guo A, Chen B, Kutschke W, Xie YP, et al. (2010) T-Tubule Remodeling During Transition From Hypertrophy to Heart Failure. *Circulation Research* 107: 520–531.
56. Calaghan S, Kozera L, White E (2008) Compartmentalisation of cAMP-dependent signalling by caveolae in the adult cardiac myocyte. *Journal of Molecular and Cellular Cardiology* 45: 88–92.